CHAPTER ONE HUNDRED THIRTY FIVE

DEPOSITIONAL EFFECTS OF OFFSHORE BREAKWATER DUE TO ONSHORE-OFFSHORE SEDIMENT MOVEMENT

Hideaki Noda*

ABSTRACT

Physical parameters controlling the development of tombolo behind offshore breakwaters are clarified on the basis of the results obtained by laboratory tests. Especially, the depositional effects are evaluated by taking a permeable type structure into account. They are wave characteristics, sediment size, the water depth where the structures are to be placed and its dimension. The amount of sand deposition behind the structures is presented by non-dimensional parameters such as the relative distances from the initial shoreline to the structure and to the breaking point of waves, the ratio of the gap width to the wave length in deep water and the ratio of the length of the offshore breakwater to the wave length in deep water.

INTRODUCTION

In considering depositional effects of an offshore breakwater by waves and currents on a beach, it is well known that offshore breakwaters act as barriers to littoral drift, blocking the natural sediment movement along the shoreline. However, sand transported from offshore sea beds by onshore-offshore sediment movement is also deposited within the protected lee of an offshore breakwater constructed on a coast where the littoral drift is not predominant,as shown by Toyoshima[2].

To gain some insight into the mechanisms, this paper deals experimentally with changes in the shoreline caused by the construction of offshore breakwaters and the amount of sand deposition within the protected lee of the breakwaters.

In addition, the distributions of the wave height and direction are measured and the currents behind the structures are observed by using floats. The results are utilized to estimate the distribution of the radiation stresses and the currents behind the offshore breakwater.

Finally, triangular-shaped groynes placed behind gaps of the structure are experimentally examined as a beach control measure.

* Professor, Department of Ocean Civil Engineering, Tottori University, Tottori, JAPAN

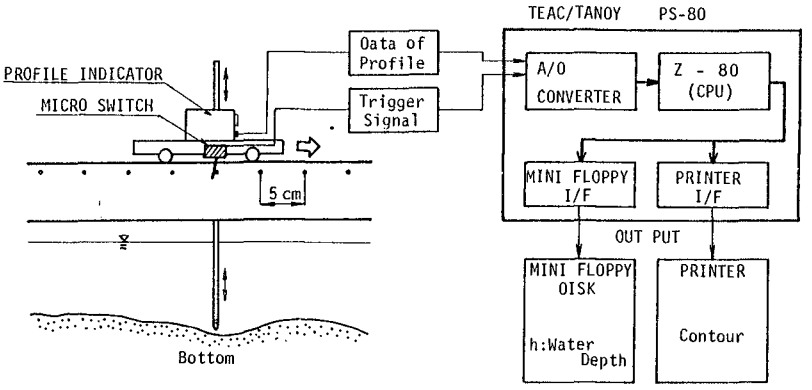

Fig. 1 Schematic diagram of measuring method for bottom configuration

Table 1 Wave conditions

	T (sec)	L_0 (cm)	H_0 (cm)	H_0/L_0	H_0/d
Type B	1.20	225	6.90	0.03	400
Type S	1.28	256	2.74	0.01	150

T: wave period, H_0: deepwater wave height
L_0:deepwater wave length, d: median diameter of sand

LABORATORY EXPERIMENTS

DESCRIPTION OF TWO MODELS

Two kinds of models were selected as the subject of the study; one was a wave flume which was designed to estimate the amount of sand transported shoreward through the permeable-type offshore breakwater and the other a wave basin which was designed to evaluate the amounts of sand transported shoreward both through the structure and from the gap between adjacent units.

The wave flume equipped with a flat-type wave generator was used; its dimension was 23 m long, 0.5 m wide and 0.6 m deep. The sediment used in the experiments was the well-sorted sand with a median diameter of 0.2 mm and a specific gravity of 2.65. The initial beach profiles constituted by this sand were uniform slope of 1/10.
The methods of the wave flume experiments are to measure the changes of the beach profiles and to estimate the volume of sand intruding into the protected area through the breakwater by using the results of the profile changes. The profiles of beaches were measured by an equipment which was developed to measure a number of depths of the bottom as soon as possible by combining a profile indicator with a personal computer as shown in Fig. 1. After the beach profile was deformed by the wave and reached the equilibrium state, the permeable-type breakwater was installed in the surf zone of the equilibrium profile and shifts in the profile were obtained until the equilibrium profile was reformed again. Table 1 is a list of wave conditions used in the experiments.

The second experiment was made by use of a wave basin measuring 12 m long, 5 m wide and 0.6 m deep. The beach was characterized by the same initial slope and sand as those of the first experiment. In order to examine the relationship between the depositional effects of the offshore breakwater and the wave behavior, the following quantities were measured: the change in shoreline shape, the amount of sand deposited in the protected lee, the distribution of the wave height and the wave direction, the distance from the breaking point to the initial shoreline and the velocity of the current behind the breakwater.

BEACH PROFILE CHANGE IN TWO-DIMENSIONAL CASE

In the experiments, two types of wave characteristics were selected to study the effect of wave action on the changes of the beach profile. As shown in Table 1, one is the B-type wave which forms a storm profile with a longshore bar and the other the S-type wave which develops a swell profile. The reason for using the two kinds of waves is to investigate the difference of sand volume deposited within the protected area by using the same waves (B-B or S-S) or the

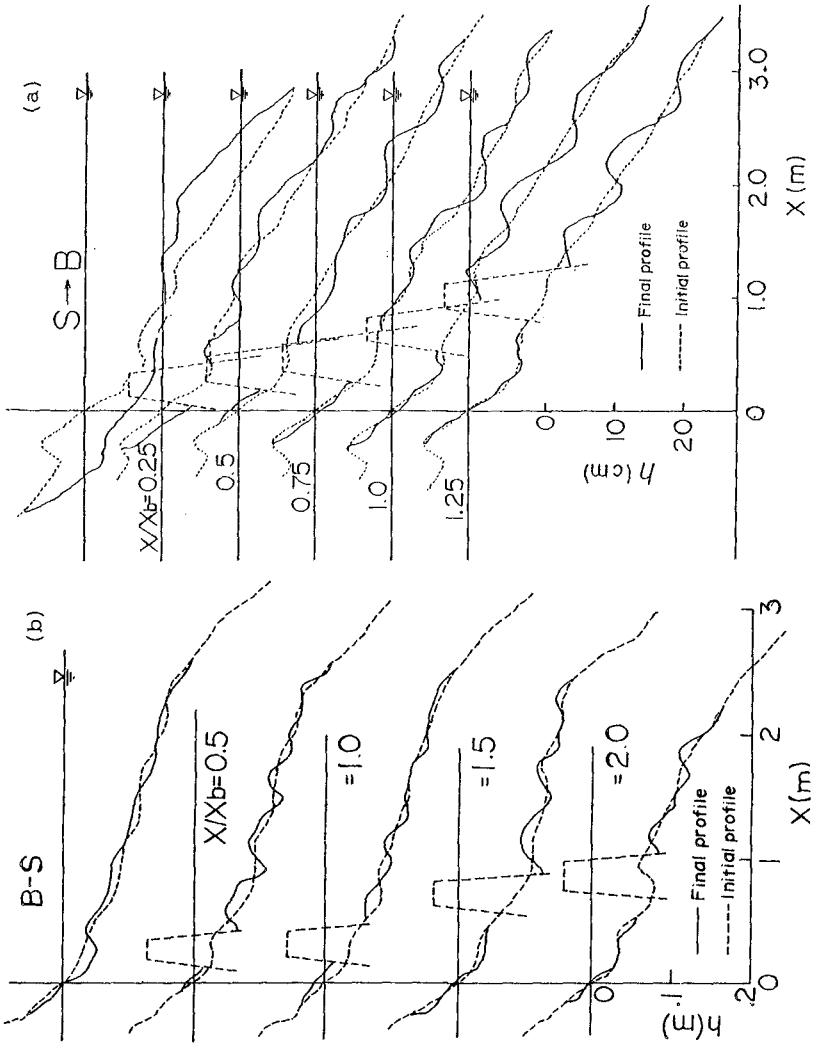

Fig. 2 Changes of beach profiles for various locations of offshore breakwater

different waves (B-S or S-B) before and after placing the structure.

Figs. 2-(a) and (b) show an example of the profile changes obtained from different waves (S-B) before and after installing the breakwater, in which X and X_b are the distances from the initial shoreline to the center of the offshore breakwater and that to the breaking point, respectively. The beach profiles at the top of this figure show the equilibrium beach profile (solid line) which was developed by the actions of the B-type wave after the equilibrium profile (dotted line) was formed by the actions of the S-type wave. As an expected result, it was found that the great recession of the final shoreline takes place in the case where there is no breakwater, while the progression of the final shoreline is caused by placing the breakwater. Fig. 2-(b) shows the similar results for B-S waves. Fig. 3 shows the relationship between the amount changes within the protected area and the relative distance of the located offshore breakwater, and V is the amount of sand deposited after placing the breakwater. In addition, the symbols shown in the upper left of this figure indicate that the experiments were carried out by using the same waves (B-B or S-B) or the different waves (B-S or S-B) before and after placing the breakwater.

This figure summarizes the depositional effects of the sediment intruding shoreward through the permeable breakwater and the amount of sand deposition depends on both the wave characteristics and the values of X/X_b. The location to maximize the amount of deposition is found when the breakwater is located at X/X_b=0.5 to 1.0 for all cases of wave types.

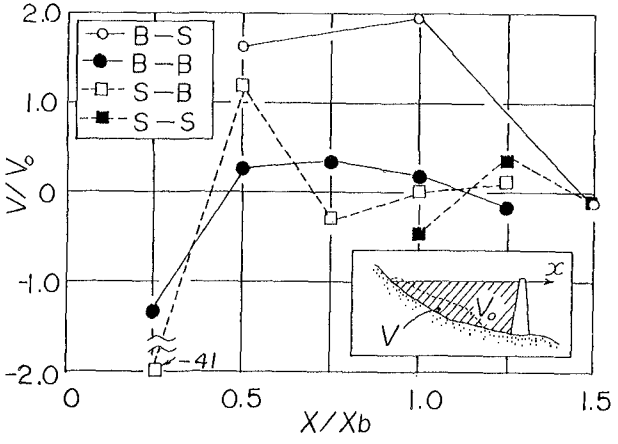

Fig. 2 Measured relationships between V/V_0 and X/X_b

CHANGE OF BEACH CONFIGURATION IN THREE-DIMENSIONAL CASE

Table 2 is a list of wave conditions used in the wave basin experiments. The method of the experiments was conducted as follows: after having the B-type waves act on the beach with a uniform slope of 1/10 and then installing the offshore breakwaters on the various locations inside the surf zone, the final equilibrium beaches were formed by the actions of the same waves. The waves used in Run A were designed to correspond to those of the two-dimensional experiment (B-B) so that quantitative evaluations can be made by comparing both data. The reason why steeper waves were used in Run B was to emphasize the depositional effects due to the onshore-offshore sediment transport, considering that the wave used in this experiment (H_0/L_0= 0.087) had a tendency to cause greater erosion.

Table 3 is a list of non-dimensional quantities related to the distance from the initial shoreline to the center of the offshore breakwater X, the length of the breakwater l_B and the width of gap between the breakwaters B. Fig. 4 shows the definition sketch for the offshore breakwaters and the beach configuration. Fig. 5-(a) and (b) are the examples of the bathymetry in the initial (t=0 hr.) and the final (t=16 hrs.) states, respectively.

Fig. 6 shows a few examples obtained in these experiments. In these figures, the solid and chain lines show the initial and final shorelines, while the various dotted and broken lines indicate the equi-depositional contour lines (unit cm) obtained from the difference between the final and initial bathymetries. These three figures result from different locations of the structure but correspond to the same wave condition (B-B). It is found that well-developed tombolos and the maximum deposition occur when the offshore breakwater is located at X/X_b=0.56. As shown by Shinohara and Tsubaki[1], bi-modal tombolo develops in the case of a short distance between the initial shoreline and the location of the structure (X/X_b=0.39).

From the condition of continuity, the total volume of sand deposition, Q, in the region abb'a' shown in Fig. 4 becomes

$$Q = Q_0 B + V l_B \tag{1}$$

where Q_0 represents the total volume of sand deposition per unit width of the gap transported through the gap and V the total volume of sand deposition per unit length of the breakwater resulting from sand intrusions through the permeable breakwater. An alternative form of Eq.(1) may read

$$\frac{Q_0}{V} = \frac{Q}{VB} - \frac{l_B}{B} \tag{2}$$

in which Q_0/V indicates the ratio of the total volume of sand deposition per unit width of the gap transported shoreward from the gap to that of sand deposition resulting from sand intrusions through the permeable breakwater. The

Table 2 Wave conditions in three dimensional experiments

	T (sec)	L_0 (cm)	H_0 (cm)	H_0/L_0	H_0/d
Run A	1.19	221	5.70	0.026	335
Run B	0.73	83	7.20	0.086	424

Table 3 Dimension and location of offshore breakwater

		X/X_b	X/l_B	l_B/L_0	B/L_0
Run A	1	0.50	0.44	0.724	0.23
	2	0.75	0.66		
	3	1.00	0.88		
Run B	1	0.39	0.44	1.93	0.60
	2	0.56	0.63		
	3	0.78	0.94		
	4		0.63	2.90	

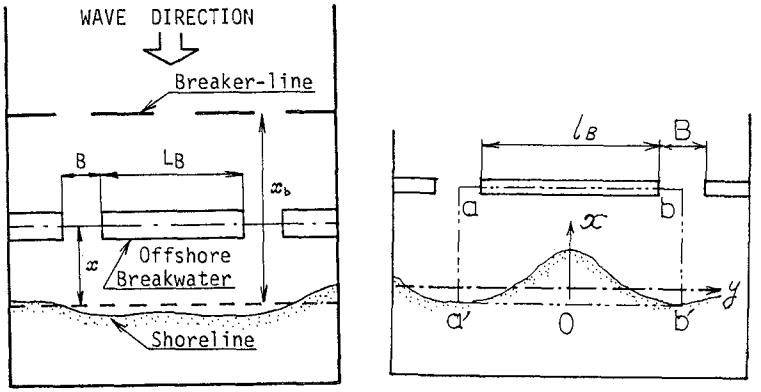

Fig. 4 Definition sketch for offshore breakwater

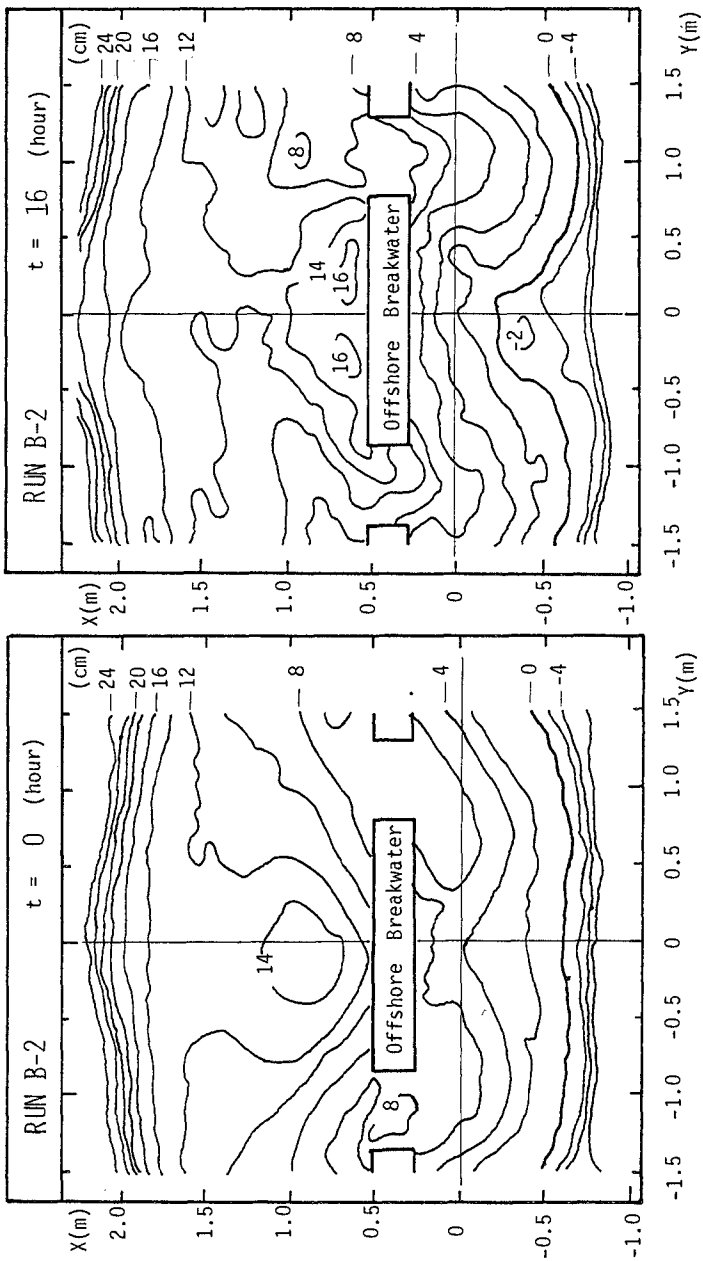

Fig. 5 Bottom topographies at the initial and final state

value of Q_0/V can be calculated by using the measured values of Q and V on the basis of Eq.(2).

Fig. 7 shows the relationship between Q/Ad and X/X_b obtained from Runs A and B, and also the same relationship between V/Xd and X/X_b obtained from the case of B-B in the two-dimensional experiments, in which A is the area of abb'a' shown in Fig. 4 and d the median diameter of sand size. A comparison of the results in Run A with those of two-dimensional experiment (B-B) having the same wave condition as that of Run A in this experiment (B-B) and the estimation of Q_0/V on the basis of Eq.(2) shows that the total amount of sand deposition per unit width of the gap transported shoreward from the gap is about three times that of the sand deposition resulting from the wave intrusion through the permeable breakwater itself. Therefore, the results suggest that the non-dimensional volume of sand deposition directly depends not only on the values of X/X_b but also on the values of l_B/B, the ratio of the length of the offshore breakwater to the width of the gap. There is, however, an exception; $Q_0/V = -0.34$ for $X/X_b = 0.75$. This fact indicates that the amount of the sand transported seaward from the gap is about three times that of the sand intruding shoreward through the permeable breakwater, although Q/Ad=0 balances the sand budget within the protected area (see Fig. 7).

Fig. 8 shows two beach profiles, one at the center of the breakwater and the other at the center of the gap for $X/X_b = 0.75$. In this figure, it is found that a large amount of sand existing near the shore-

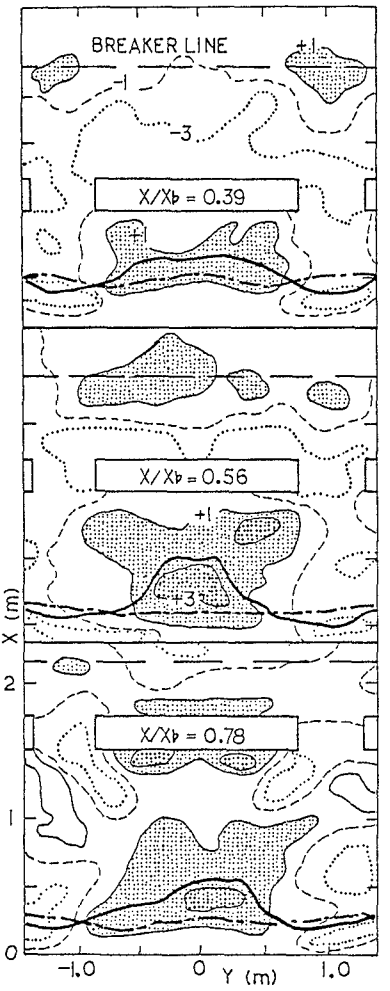

Fig. 2 Changes of shoreline and bottom configuration at various locations of offshore breakwater

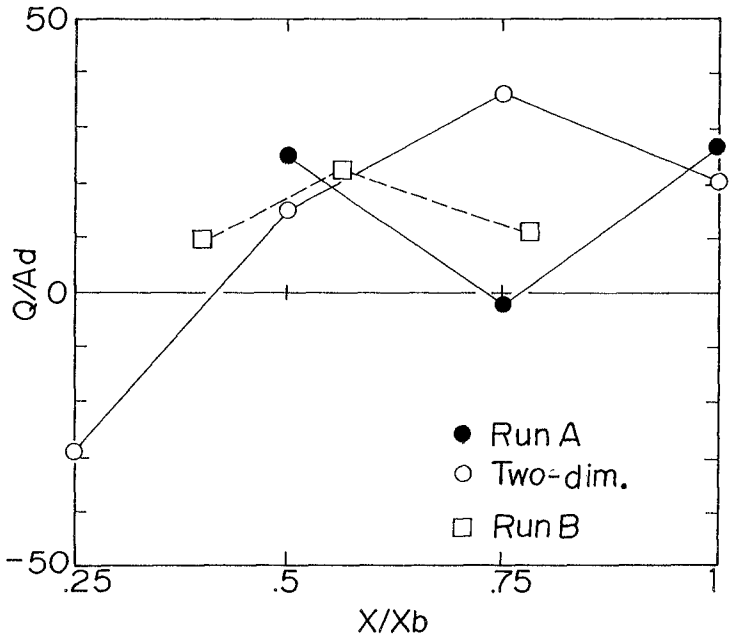

Fig. 7 Relationship between Q/Ad and X/X_b

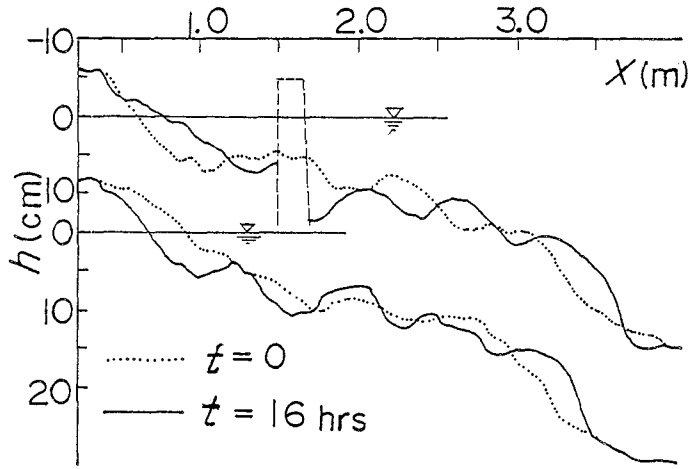

Fig. 8 Changes of beach profiles

line behind the gap is taken away by waves and currents, since the progression of the shoreline takes place and a tombolo is developed near the center of the breakwater but the scour of its lee just behind the offshore breakwater occurs and the regression of the shoreline behind its gap is greatly eroded.

MEASUREMENT OF WAVE AND CURRENT CHARACTERISTICS

An attempt was made to investigate the mechanism of sand deposition due to the onshore-offshore sediment transport, the measurements of wave parameters and the resulting currents in the protected area were made under the condition of Run B-2 in which the maximum amount of sand deposition in the area of the protected lee was observed.

Fig. 9 shows the results of measured wave height and direction in various locations. In this figure, the local variation of wave height is expressed by the ratio of wave heights measured in each location, H, to the incident wave height H_I. Both the direction and the length of each solid line segment with an arrow head represent the direction of waves and the ratio H/H_I, respectively. Each contour line corresponds to a certain value of this ratio. The following may be found from this figure : 1) a partial clapotis is developed in the area seaward of the offshore breakwater, 2) diffraction of waves is observed in the vicinity of the gap, and 3) transmitted waves intruding through the breakwater are recognized just behind the offshore breakwater.

By introducing a rectangular co-ordinate system (x,y), in which the orientation of the co-ordinate system is chosen so that the x-axis lies roughly perpendicular to the initial shoreline as shown in Fig. 10, the radiation stresses in the measuring points of the wave height are expressed by

$$\begin{pmatrix} S_{xx}, & S_{xy} \\ S_{yx}, & S_{yy} \end{pmatrix} = E \begin{pmatrix} n\cos^2\theta + n - 0.5, & -0.5\, n \sin 2\theta \\ -0.5\, n \sin 2\theta, & n\sin^2\theta + n - 0.5 \end{pmatrix} \quad (3)$$

where θ is the angle between the wave direction and x-axis, n the ratio of the group velocity to the wave velocity and E the wave energy. In addition, the non-dimensional friction terms (R_x, R_y) related to the wave-induced currents are given by

$$R_x = -\frac{1}{\rho g h}\left(\frac{\partial S_{xx}}{\partial x} + \frac{\partial S_{yx}}{\partial y}\right)$$
$$R_y = -\frac{1}{\rho g h}\left(\frac{\partial S_{xy}}{\partial x} + \frac{\partial S_{yy}}{\partial y}\right) \quad (4)$$

in which ρ is the density of water, g the acceleration of gravity and h the water depth. The radiation stresses based on Eq.(3) can be calculated by using the measured wave

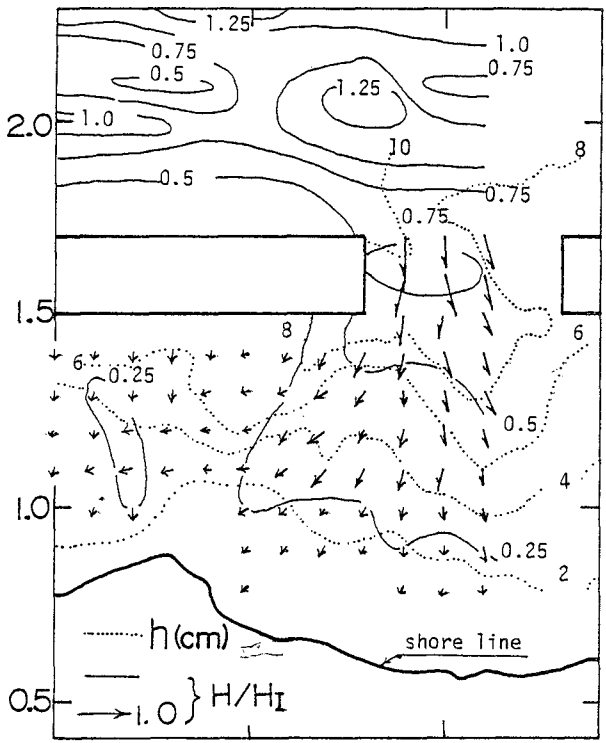

Fig. 9 Distribution of wave height expressed by the ratio of H/H_I

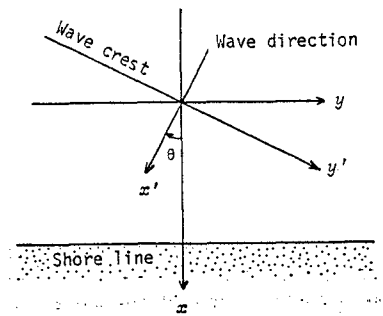

Fig. 10 Definition sketch of co-ordinate system

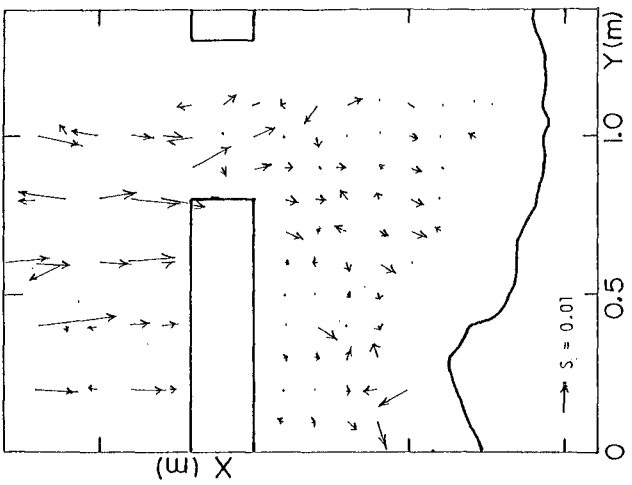

Fig. 11 Distribution of S esimated by radiation stresses

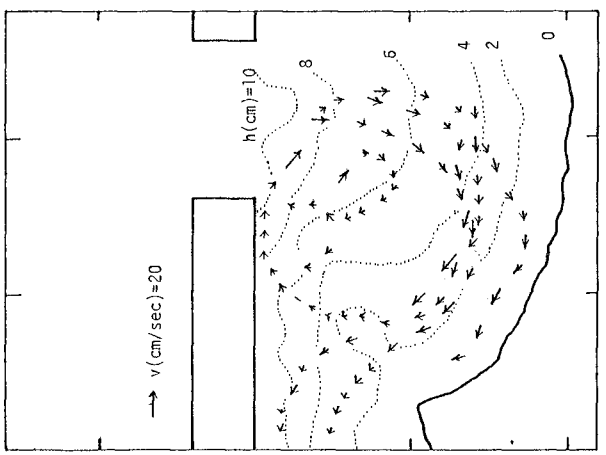

Fig. 13 Current pattern measured by float

parameters and then the friction terms in Eq.(4) can be also computed based on the numerical results of the radiation stresses calculated above and by use of a finite difference numerical method.

Fig. 11 describes the spatial distribution of the vectors S estimated on the basis of Eq.(4), in which the magnitude and direction of the vector S are calculated by $S = (R_x^2 + R_y^2)^{1/2}$ and $\theta_s = \tan^{-1}(R_y/R_x)$, respectively. Fig. 12 shows the observed current pattern in which the velocity and direction of currents are expressed by a segment of a solid line with an arrow head. Comparison of Fig. 11 with Fig. 12 suggests that the circulation estimated in Fig. 11 shows a similar pattern to that of the wave-induced currents in the shoreward region of the gap. It seems that such a numerical method serves for estimating wave-induced currents in the protected area. Furthermore, it appears that the circulation observed in Fig. 12 contributes to the sand accumulation within the protected lee of the breakwater, the development of tombolo and the retreat of the shoreward area of the gap by onshore-offshore sediment movement.

SOME MEASURES FOR EROSION IN LANDWARD AREA OF GAP BETWEEN OFFSHORE BREAKWATERS: AN ATTEMPT

Since the offshore breakwater had such a defect that the shoreward area of gap between adjacent units was eroded in all the cases of the experiments, some measures were tested to protect the area from landward retreat. One of the measures was to place triangular-shaped jetties in the area, considering that the jetty is effective from the view-point of preventing the circulation of currents which appears to develop tombolo.

Experiments were made by using the same wave basin as mentioned in the foregoing section. The wave condition was the same as Run B in three dimensional case, and the locations where the offshore breakwaters were placed were the same as Runs B-2 and B-3 (see Tables 2 and 3). Fig. 13 shows a schematic diagram of the triangular-shaped jetty which was placed behind the gap of the offshore breakwaters. Here, X_j is a distance from the initial shoreline (chain line) to the head of the jetty.

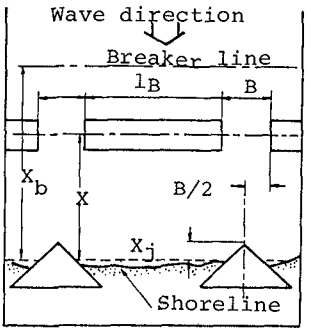

Fig. 13 Schematic diagram

Fig. 14 shows the changes of

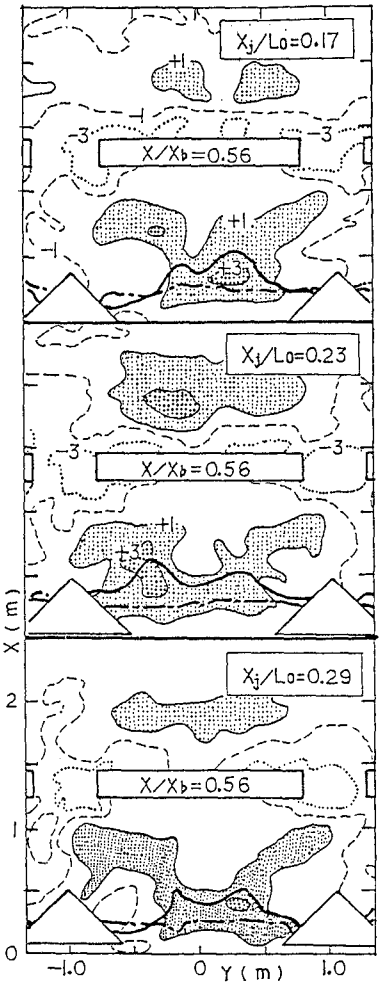

Fig. 14 Comparison of changes in shoreline and Bottom configuration for the cases with jetty

the shoreline form and the bottom topography for various values of X_j/L_0 under the same wave condition as Run B-2 and X/X_b=0.56.

Comparison between these figures and the middle figure in Fig. 6 (no jetty) indicates that the landward retreat takes place in the tip part of tombolo, while the scour in the surroundings of the gap and the offshore breakwater is reduced considerably. Furthermore, a remarkable fact is that the regression of shoreline in the area can be prevented when the jetties are placed at X_j/L_0=0.23.

Fig. 15 summarizes the results of the sand volume deposited in the protected area, Q/Ad vs. X_j/L_0. In the case of X/X_b=0.56, the sand volume deposited in the area decreases slightly with increase in the values of X_j/L_0. Furthermore, a noticeable result is that the non-dimensional sand volume in all cases with the jetty is small compared to those without the jetty, while the landward retreat of the shoreline behind the gap can be prevented in the former cases. Contrastly, in the case of X/X_b=0.78, the sand volume for the experiments with the jetty always exceed that for the experiments without the jetty.

It is clear that an appropriate location for constructing jetties is largely confined by wave characteristics, width of gap, length and location of the offshore breakwater. It also appears that the relative location of the offshore breakwater and jetty plays an important role in the development of the current pattern.

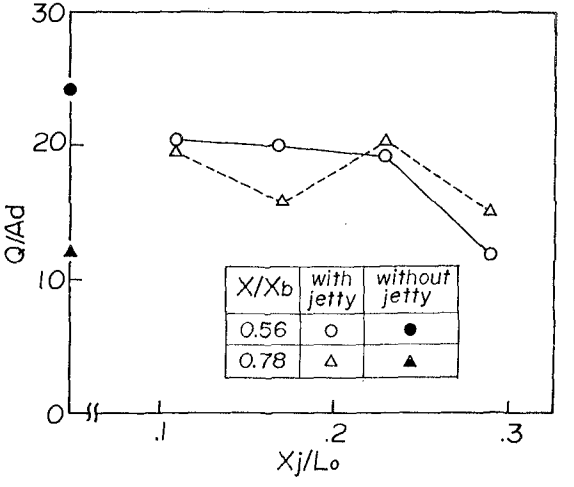

Fig. 15 Relationship between Q/Ad and X_j/L_0

CONCLUSION

The following may be concluded from the laboratory tests on the depositional effects of the offshore breakwater due to onshore-offshore sand transport:

1. the optimum locations at which the effective deposition of sediment behind the offshore breakwaters develops are at $X/X_b=0.5$ for B-type waves and at $X/X_b=1.0$ for S-type waves in the results of two-dimensional tests.

2. there is found no sand that intrudes shoreward through the permeable type of the offshore breakwater when the structures are placed seaward beyond the breaker line of waves. On the contrary, a large amount of sands may be carried away offshore when the offshore breakwaters are placed near the shoreline.

3. the total amount of sand deposition per unit width of the gap transported shoreward from the gap is about three times that of sand deposition intruding through the permeable breakwater, when the dimensions and location of the breakwaters are chosen appropriately.

4. the current pattern induced by the wave action behind the structures may be predicted by applying the concept of radiation stresses.

5. construction of the triangular jetties may be utilized as one of the measures to prevent the scour in the surroundings of the breakwaters or the landward retreat behind the gap.

ACKNOWLEDGMENTS

The author would like to express his appreciation to Mrs. K. Noda, Y. Shimizu and N. Kurose for their assistance in the laboratory experiments, and expresses appreciation for financial support of the Grant-in-aid for Scientific Research of Ministry of Education.

REFERENCES

1) Shinohara, K. and T. Tsubaki: Model study on the change of shoreline of sandy beach by the offshore breakwater, Proceedings of 10th Coastal Engineering Conference, 1966, pp.550-563.

2) Toyoshima, O.: Design of a detached breakwater system, Proceedings of 14th Coastal Engineering Conference, 1974, pp.1419-1431.